

ROCK STRENGTH, BRITTLENESS AND BLAST FRAGMENTATION

N. D. Fowkes*, G. C. Hocking †, D. P. Mason‡

Industry Representative

T. R. Stacey§

Study group participants

Z. Dlamini, T. Motsepa, S.O. Ojako, A. Nour, V. Magagula
Sibabalwe Mdingi, Busisiwe Mncube, Martins Arasomwan

Abstract

The problem considered by the MISG was that of rock sizes obtained during targeted blasting. The goal is to determine the average size distribution of rocks given the conditions and explosives used. The Kuz-Ram model is an empirical model that has been used over the past 25 years for estimating the mean fragment size and distribution. The model is inadequate because it contains an unknown factor that may vary by an order of magnitude. However, we also believe it is conceptually flawed because important rock properties such as rock brittleness and yield strength are not accounted for ‘at first order’ and the model result is dimensionally inconsistent.

During the MISG a dimensional analysis was performed in an attempt to redress this error. In addition, two new models of the dynamic fracturing process were derived; a ‘breaking spring model’ and a continuum model. The breaking spring model is shown to display the ‘correct’ stress/strain behaviour for ductile rock types, but needs modification to handle hard rocks. Initial work on the continuum model seems to give some promise of explaining the rock behaviour during blasting.

*Mathematics Department, University of Western Australia, Crawley, WA 6009, Australia *e-mail: neville.fowkes@uwa.edu.au*

†Mathematics and Statistics, Murdoch University, Australia *e-mail: g.hocking@murdoch.edu.au*

‡School of Computer Science and Applied Mathematics, University of the Witwatersrand, Private Bag 3, WITS 2050, Johannesburg, South Africa. *e-mail: David.Mason@wits.ac.za*

§School of Mining Engineering, University of Witwatersrand, Johannesburg, South Africa, *e-mail: Thomas.Stacey@wits.ac.za*

1 Introduction

Knowing the size of the fragments produced during rock quarry blasting is of major engineering importance. If the rocks are to be used for some downstream operation (e.g. building a breakwater) then they need to fit within certain size parameters. If they are just to be removed, then they need to be of a suitable size for efficient removal.

There is a standard model for size estimation referred to as the Kuz-Ram model after its creators Kuznetsov, Rammler and Rosin, with the name proposed by Cunningham [1] in the 1980's. The limitations of the model are well known, see Cunningham [1], and Kulatilake [2] but experienced engineers recognise the problems and are able to adapt. Nevertheless a better model would hopefully lead to more consistent results not so dependent on experience.

Richard Stacey asked the MISGSA 2016 to investigate the possibility of producing a better estimate based on Tarasov and Potvin rock brittleness ideas. There have been many proposed definitions for rock brittleness but the Tarasov index is based on relatively standard stress vs. strain laboratory tests on rock and energy exchange arguments, and so is particularly suitable in the present context, see Tarasov and Potvin [7], and Tarasov and Randolph [6].

The outcomes of the MISGSA investigations are presented here. In Section 2 we present the Kuz-Ram model and briefly describe the Tarasov brittleness index ideas (and the related rupture energy index), and then go on to use scaling arguments to suggest a possible empirical formula which we believe may provide for better fragment size estimates. Rigorous testing would be required to check if this were so, but the principle of having a dimensionally correct formula is important and should be adhered to even if the form is different to that proposed herein.

There have been many mechanistic models proposed to describe both crack propagation and fragmentation; an excellent recent review of this material was produced by Zhang and Zhao [4]. Such models attempt to track the physics of the fragmentation process for specific blast layouts in simple known cases. In Section 4.1 we produce a new mechanistic model for fragmentation. The model is based on a breaking springs analogue and closely ties in with the Tarasov brittleness index observations; in this way it differs from previous models. The various features associated with the stress/strain experiments have been identified and it is hoped that this model will produce useful results for dynamical simulations of the fragmentation process. In Section 5 a second (continuum) mechanistic model is presented based on state change ideas. This continuum model again ties in with the Tarasov work and results in a more detailed description of the fragmentation process. Such a model, when fully developed, may enable more accurate estimates to be made for the fragmentation process. Conclusions will be drawn in Section 6.

2 Empirical Models and Background

2.1 The standard Kuz-Ram model

In general terms with rock blasting in quarries more explosive leads to smaller fragments and tougher rocks result in larger fragments as born out in field tests. There is a standard model (the Kuz-Ram model) that has been used in the mining industry for 25 years for estimating fragment size and distribution. This model determines the mean fragment size as

$$x_m = AK^{-0.8}Q^{1/6}\left(\frac{115}{RWS}\right)^{\frac{19}{20}}, \quad (1)$$

where x_m is the mean particle size (m), K is the powder factor (kg explosive/ m^3) and Q is the mass of explosive in a single hole (kg). RWS is the relative weight strength of the explosive used relative to TNT, 115 being the RWS of TNT, and A is a ‘rock characterisation factor’, varying over the range 0.8 to 22.

This rock characterisation factor A estimates the effect of geology on fragmentation, and is defined as

$$A = 0.06(RMD + RDI + HF), \quad (2)$$

where RMD is the rock mass description, which takes into account the rock condition (powdery/friable) and the distribution and state of joints, RDI is the density influence and HF is the hardness factor. This takes into account the elastic modulus and compressive strength of the rock. In addition, a multiplicative ‘correction factor’ is often introduced to bridge the gap between observed and calculated on-site results (typically in the range 0.5 – 2). For more details see Cunningham [1].

In addition to the above formulae there is the fragment distribution formula

$$R_x = \exp[-0.693(x/x_m)^n] \quad (3)$$

with $n = 0.7 - 2$. Research has shown that this model underestimates the contribution of fines in the distribution [2].

The advantage of these formulae is that they are simple and require little on-site data. However, they do not take into account specific features of the blast (rock type, bore hole spacing, geometry of the site...). Mechanistic models have been developed that aim to quantify such effects, but such models necessarily require more specific input from the site, see Zhang and Zhou[4], and are thus less likely to be used in practice.

The Kuz-Ram formula is incorrect as a dimensional statement and was evidently obtained as a best fit using available data and the chosen parameters. Subsequent improvements were achieved by introducing modifications to the basic result. Of particular concern is that rock properties, which are clearly of central importance for fragment size determinations, appear in the form of a rock parameter A which

is really an ‘add on’; in fact A has been seen to vary over a very large range (1 to 22) which clearly indicates the central role rock properties play.

Our aim in Section 3 is to produce a better basic model which includes the most important parameters (and in particular the rock properties) in a dimensionally consistent way; the results obtained using this model should be more robust and thus require less adjusting to take into account secondary features.

It should be understood that any simple formula of the Kuz-Ram type will have restricted applicability. For example there is an inbuilt assumption that the explosive distribution and design is sensible/standard; so that the explosive energy released is used for cracking the rock rather than producing powder. Under such circumstances one might hope that the formula would provide useful guidance.

2.2 The Tarasov/Potvin brittleness index

There are many definitions of ‘brittleness’ but in context it is the index introduced by Tarasov and Potvin [7] that has most relevance to fracturing. The brittleness ‘index’ defines the extent to which a rock is ‘brittle or hard’ (Class II) or ‘ductile’ (Class I) and, as defined by Tarasov and Potvin, is based on the standard stress/strain laboratory test for rocks. Granite would be regarded as a brittle material and sandstone as a ductile material. Typical stress vs. strain results for a ductile material are shown in Figure 1 (Left), and for a brittle material in Figure 1(Right). The work performed on the sample by the externally applied compressive stress is the area under the stress/strain curve up to the final state and one can identify the various energy storage components as areas on this figure.

With increasing externally applied stress both solids behave elastically until the yield/peak stress Y is reached. After Y ‘stress control is lost’ and the sample ruptures. If C is the final stress state then the red area represents the ‘elastic energy stored’ (ie remaining in the sample) and the grey area represents the rupture energy (energy used to rupture the material). For ductile (Class I) materials external work is needed to cause this rupture and the rupture energy is positive. For brittle (Class II) materials some of the stored elastic energy is used to rupture the material (the grey area), some is retained as elastic energy in the material (the red area); the rupture energy is negative in this case. Additionally some of the initially stored energy at peak stress Y is released in the form of heat etc. (the yellow area). For more details see Tarasov [7].

Note the very different shape of the stress/strain curve of the ductile and brittle materials after the yield stress Y is exceeded. The stress/strain curve for the ductile material has the familiar negative slope (corresponding to a negative post-peak modulus) associated with the plastic behaviour of metals. The stress/strain curve for a brittle material on the other hand ‘folds back’ on itself and the curve slope remains positive (corresponding to a positive post-peak modulus) after a small transition.

Thus in the ductile material external work needs to be performed on the sample to produce rupture, whereas in the brittle material case some of the elastic energy

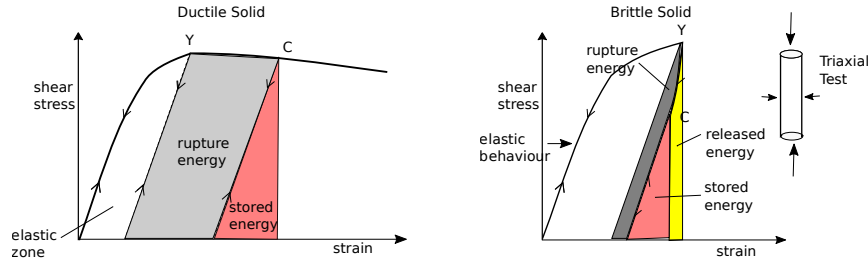


Figure 1: Triaxial compression tests on samples: Left: Class 1 (ductile/plastic) solids, Right: Class 2 (hard/brittle) solids.

already stored in the material during compression is used to rupture the sample. Also ‘excess’ energy is released in the form of heat, vibration etc. so the process can be ‘self sustaining’, see Section 5. The important thing to notice is that all such components can be associated with specific areas under the experimentally obtained stress/strain curve for the quarry rock.

As one might expect, the brittle stress/strain curve in the brittle rock case under conditions close to peak-stress can only be produced by using careful experimental techniques. What happens normally is that the stress level dramatically (and uncontrollably) reduces as the peak stress level Y is approached, while the strain increases (the rock slab snaps forward). Technically speaking the pre-yield stress/strain solution becomes unstable close to Y and small perturbations cause a transition to the other post-peak stable solution branch.

Real rocks are neither totally brittle nor totally ductile, but based on the above stress/strain curves Tarasov and Potvin defined the ‘brittleness index’ K_1 as the ratio of the elastic energy withdrawn from the material during the failure process to the rupture energy (ie energy required to produce rupture); if this ratio is greater than unity then the process will be self sustaining (the brittle case), whereas if it is less than unity then energy would need to be supplied to sustain the rupture process (the ductile case). The sign of the brittleness index dramatically effects the dynamic fracture behaviour and this will be discussed later.

In the present fragmentation context, however, we are interested in knowing what fraction of the work done by the explosive force on the material particle is used to rupture the rock; we thus define ‘the rupture energy index’ (β) as the ratio of the rupture energy to the external energy input (or work done on a material particle by the explosive force). Thus *the rupture energy index* is defined as

$$\beta = \pm \frac{\text{grey area}}{\text{white area} + \text{grey area}},$$

where the negative sign corresponds to Class 2 brittle rocks where internal elastic energy is used to fragment the sample and the positive sign corresponds to the case

in which external work needs to be performed to fragment the sample (areas relate to Fig. 1). The rupture energy index and the fragmentation size distribution can be obtained using triaxial stress/strain experiments.

The underlying assumption involved in work to follow is that the experimental stress/strain results mirror what will happen to material particles under quarry blasting conditions, so that the index β determines the proportion of explosive energy used to rupture the rock and in particular determines the effect of rock brittleness on quarry blasting. We present three possible fragmentation models with different emphases: a scaling model, a spring model, and a continuum model.

3 A Scaling Fragmentation Model

The aim is to improve on the Kuz-Ram model using dimensional analysis. An outline of the method of dimensional analysis and details in the derivation of the results presented in this section are given in Appendix A 6.

Dimensional analysis proceeds by identifying the n (say) primary physical parameters and then determining the possible combinations of these parameters that are required to produce the desired dimensional quantity. The Buckingham Pi Theorem not only asserts this dimensional consistency result but also determines the number of dimensionless products that can arise as being $p = n - k$, ($n \geq k + 1$) where k is the number of independent physical dimensions involved. In our present case the aim is to produce an expression for the mean size of a fragment (dimension L) produced by an explosive charge. One might expect the explosive charge per unit volume per time and fracturing rock properties such as yield strength and brittleness to be primary parameters. Other rock parameters such as the Young's modulus or elastic wave speed might also be important and could be required to produce a dimensionally consistent result.

Model parameters

We assume for a start that the following parameters are primary:

- Mean fragment size x_m : dimensions L
- Yield stress Y : dimensions $\frac{M}{T^2L}$.
- Energy per unit time per unit volume due to explosive charge \mathcal{E} : dimensions $\frac{M}{T^3L}$.
- The rupture energy index β : dimensionless.

Based on the previous section we assume that the available energy for fragmentation is $\beta\mathcal{E}$: dimensions $\frac{M}{T^3L}$; this enables us to reduce the number of physical parameters.

- Speed of propagation of the elastic wave (primary wave) C_P , with dimensions $\frac{L}{T}$

We thus have four parameters and three physical dimensions L, M, T , so that just one dimensionless product can arise according to the Buckingham Pi Theorem. The possible combinations for determining x_m are:

$$x_m = AY^a(\beta\mathcal{E})^bC_P^c = A \left(\frac{M}{T^2L} \right)^a \left(\beta \frac{M}{LT^3} \right)^b \left(\frac{L}{T} \right)^c$$

and dimensional compatibility occurs provided:

$$\begin{aligned} L : & \quad 1 = -a - b + c, \\ M : & \quad 0 = a + b, \\ T : & \quad 0 = -2a - 3b - c. \end{aligned}$$

Thus $a = 1, b = -1, c = 1$, which gives

$$x_m = A \frac{YC_P}{(\beta\mathcal{E})}, \quad (4)$$

where $C_P = \sqrt{\frac{E(1-\nu)}{\rho(1+\nu)(1-2\nu)}}$; E is Young's modulus, ν Poisson's ratio and ρ is the density.

Note that this formula is dimensionally correct and includes the important rock properties in a way that seems intuitively correct. For example the fragment size is anticipated to be inversely proportional to the effective energy release rate per unit volume and the fragment size varies inversely with the rupture energy index as observed. In the limit as $\beta \rightarrow 0$ the fragmentation energy goes to zero, and the particle size thus goes to infinity. The $\beta = 0$ case separates out brittle fracture from ductile rock failure.

It should be recognised that the above result presumes that the four physical parameters selected are the primary parameters determining fracture. If a different list was selected then a different result would be obtained, for example

$$x_m = \frac{Y^{3/2}}{(\beta\mathcal{E})\rho^{1/2}}$$

is also a dimensionally correct combination ¹. The preliminary results obtained in Section 5 do however suggest that the C_P term is a primary physical parameter and that the density dependence is correctly absorbed into the C_P term.

Such issues of parameter choice would be settled if (a) the correct defining equations were available and dimensionless products were obtained by scaling these

¹The significant difference from the previous result is that in one case $x_m \propto Y^{3/2}$ whereas in the other case $x_m \propto YE^{1/2}$.

equations (this is attempted in Section 5), and (b) if available data supports the results obtained.

There are many other features/parameters of a quarry explosion that are not included in the above scaling exercise that are known to increase fracturing efficiency, but we think of these as being of secondary importance. For example it is known that a time delay between charge ignition at different locations improves efficiency; if B is the spacing then an enhancement in effectiveness can be achieved if a delay of about $\Delta t = B/C_P$ is used (to avoid interference). According to the Buckingham Pi Theorem each additional parameter will result in an additional dimensionless product. For example the spacing effect introduces two new physical quantities Δt and B , and therefore two dimensionless products can be included in (4) as

$$x_m = A \left[\frac{Y C_P}{(\beta \mathcal{E})} \right] \text{fn} \left(\frac{C_P \Delta t}{B}, \frac{Y}{\beta \mathcal{E} \Delta t} \right),$$

with the function $\text{fn}(\cdot)$ scaled to unity under most efficient conditions so as not to modify the value of A . Additionally the formula can be adjusted to take into account the effect of hole spacing B compared with rock joint spacing J ; in this case (4) would be modified as

$$x_m = A \left[\frac{Y C_P}{(\beta \mathcal{E})} \right] \text{fn} \left(\frac{B}{J}, \frac{C_P \Delta t}{B}, \frac{Y}{\beta \mathcal{E} \Delta t} \right).$$

This approach of adding in additional factors in a dimensionally consistent way could be employed to improve the primary result *after this result is established*. The actual determination of such functions would require data fitting so that it would be impractical to deal with more than one additional factor.

The important question is whether the result (4) is likely to be more reliable than the Kuz-Ram model? The answer is “yes”, providing the identified parameters are primary. This can only be decided observationally: if the model is better then the parameter A will vary little with rock type and explosive arrangement, assuming a reasonable, standard charge pattern.

4 Mechanistic Models

The fragmentation process is complex. The application of an external force to a brittle rock causes micro cracks to extend and join up with other micro cracks forming a discernible crack which continues to extend (subcritically) as the applied stress increases until the crack reaches a critical length. At this stage the elastic energy released due to crack extension exceeds that required to form the crack surface, so the crack extends spontaneously, moving with a speed of roughly 2/3 of the speed of travel of Rayleigh waves for the material. An excellent account of single crack extension can be found in Broberg [3]. This release of elastic energy stops the growth of other cracks that may have been in the process of extending

so that usually a single crack dynamically extends during this phase. The further application of the external force results in a transition from ‘single fracturing or splitting’ to ‘multiple fracturing or pulverisation’, and this later process seems to be distinctively different, occurring much more slowly and driven by strain rate, see Li et al [5]. Many models have been developed to try to describe this later stage but the process is not well understood. An excellent recent review of the literature can be found in Zhang and Zhao [4].

In view of the above results it seems that an understanding of single crack extension is unlikely to lead to an understanding of fragmentation. In the next subsection we will examine a spring model which may lead to a better description of the dynamic process. A second continuum model based on ‘state change’ ideas is presented in Section 5. In both cases the models developed are based on Tarasov’s brittleness index ideas.

4.1 A breaking springs model

The formation of cracks in a material subjected to stress is likened to the breaking of springs when subjected to stress levels that exceed their breaking strength. In this analogy model, intact rock corresponds to intact springs and cracks correspond to broken springs, with the easily breaking springs corresponding to weaker material pathways through the solid material. The spring situation envisaged is depicted in Figure 4.1. Also the situation envisaged is one in which the quarry consists of material represented by the springs and the applied force in the spring arrangement is associated with the gas pressure associated with the explosion. In reality this force is ‘internal’ but here we treat it as an external force applied at the edges of the quarry. The idea behind this work is simple: if this setup leads to stress/strain relations similar to Class I and II models, and the various parameters can be directly related to the material parameters (yield strength, brittleness, Young’s modulus) then the model may be usefully extended to handle dynamic situations such as fragmentation. Of course this will only work if detailed cracking mechanics is not ‘controlling’ as suggested above.

Here we demonstrate with a one dimensional model, but in principle it is possible to do this in three dimensions with directional behaviour of the springs. Initially there are n_0 springs that are stretched by an external force \mathcal{T}_{ext} . As a demonstration, we assume the individual springs have the same spring constant (k), so that

$$T_s = kx, \tag{5}$$

where x is the extension, but have different breaking strengths T_s^{crit} .

Spring breakage distribution

If we assume a normal distribution for (individual spring) breakage tension with average breaking tension \bar{T}_s^{crit} and with standard deviation, σ , then we have the

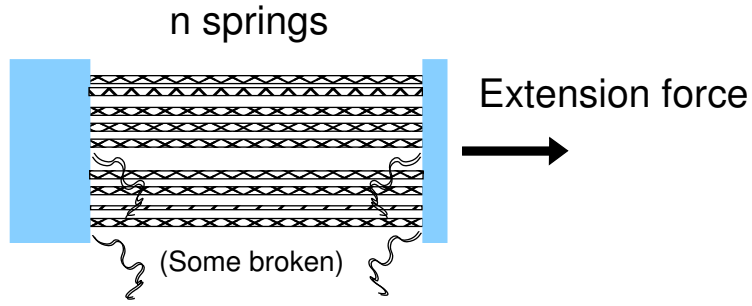


Figure 2: The spring analogue to rock fracture. The n springs are subjected to an external force \mathcal{T}_{ext} . Individual springs are therefore subjected to an external force of $T_s = \mathcal{T}_{ext}/n$. Some break and the remaining springs bear the load.

frequency distribution given by (see Figure 3)

$$f = \frac{1}{\sqrt{2\pi}\sigma} \exp \left[- \left(\frac{(T_s^{crit} - \bar{T}_s^{crit})^2}{2\sigma^2} \right) \right].$$

With such a breakage distribution the application of a (individual) tension of T_s

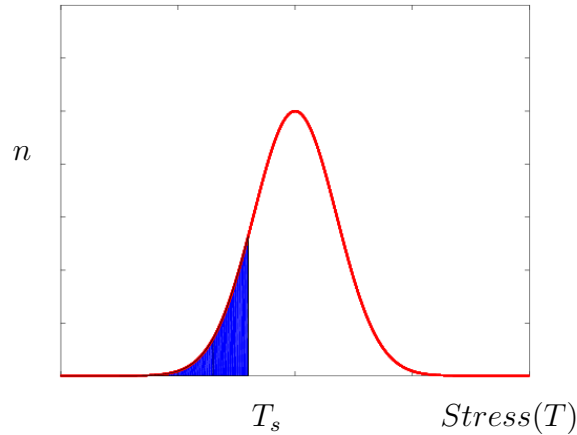


Figure 3: An example of the breakage distribution of springs, where n is the number of bonds (springs) that will break at the given value of stress (T). All springs with breakage stresses in the shaded region, i.e. $T < T_s$ are assumed to break. The load is then re-distributed among the remainder.

will cause all springs with breaking tensions less than T_s to break, so strings in the shaded area in the figure will have broken, leaving the remaining n springs to bear the load.

Multiplying the individual tension vs. stretching relationship (5) by the number of intact springs n we obtain the global stress vs. strain relationship

$$nT_s \equiv \mathcal{T}_{ext} = (nkl_0) \frac{x}{l_0} \equiv E_{eff} \frac{x}{l_0};$$

thus the effective Young's modulus of the material is defined in terms of the spring constant k and the number of springs n , explicitly

$$E_{eff} = E_0 \left(\frac{n}{n_0} \right). \quad (6)$$

We now identify the number of surviving springs supporting the load as:

$$\frac{n}{n_0} = 1 - \int_0^{T_s} f(T_s) dT_s,$$

which gives us an explicit expression for the effective Young's modulus as

$$E_{eff} = E_0 \left[1 - \int_0^{T_s} f(T_s) dT_s \right] \quad (7)$$

which integrates to give

$$E_{eff}(T_s) = E_0 \left[1 - \text{Erf} \left(\frac{T_s - \bar{T}_s}{\sqrt{2\pi}\sigma} \right) \right], \quad (8)$$

in the normal distribution case. Thus the effective Young's modulus is reduced due to spring breakage and can be explicitly determined as a function of the applied stress. The resulting global stress/strain result is given by

$$\mathcal{T}_{ext} = nT_s = E_0 \left[1 - \text{Erf} \left(\frac{T_s - \bar{T}_s}{\sqrt{2\pi}\sigma} \right) \right] \frac{x}{l_0}. \quad (9)$$

Results

The results of an example case are displayed in Figure 4. The stress-strain curves start bending as the stress enters the breaking stress region and asymptote to a T_s with all springs broken. The rate of approach to this asymptote is dependent on the width of the breaking stress distribution σ .

It should be noted that if the applied stress is cycled then no further springs are broken as the stress is reduced and subsequently breakage will reoccur when stress levels again exceed the previous maximum stress level, as is displayed in Figure 4. When the applied stress level is reduced to zero there will be a residual displacement which will be added to by successive increases in stress level above the previous maximum level. This does coincide with observations.

One can associate rock characteristics with spring model parameters. The effective Young's modulus is as indicated earlier (6). The yield strength is identified

with the asymptote and the brittleness index relates to the areas in Figure 4. However, some features of the stress/strain results are not duplicated. The stress/strain curves dip after the yield strength is reached. Also while the shape is right for Class II brittle rocks, Class I models are not covered and it may be that the elastic constants need to be normally distributed as well as the breakage distributions.

Hopefully the inadequacies can be addressed and if so the next stage will be to extend the results to cover the dynamics. It is a simple matter to introduce momentum by having springs with a distributed mass. Such a model should lead to a better understanding of the effect of the quarry boundaries on fragmentation.

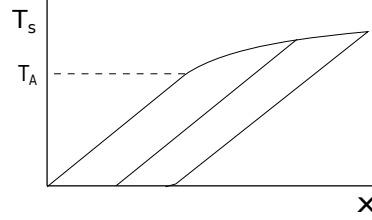


Figure 4: Stress vs strain results for the springs model. The 2nd and 3rd parallel lines with positive slope correspond to the curve if the stress is reduced from two different points.

Simulations for random distributions

The above results were obtained for a normal distribution of breaking tension but extend to any distribution of breaking tensions. For example, if one uses a randomly generated distribution with prescribed mean and variance then for the cases shown in Figure 5 the results obtained are as shown in Figure 6.

As would be expected given the analytic results above a narrow breakage distribution results in a narrower/sharper transition from elastic to non-elastic post yield condition behaviour. Note that these results do not provide a model of Class I

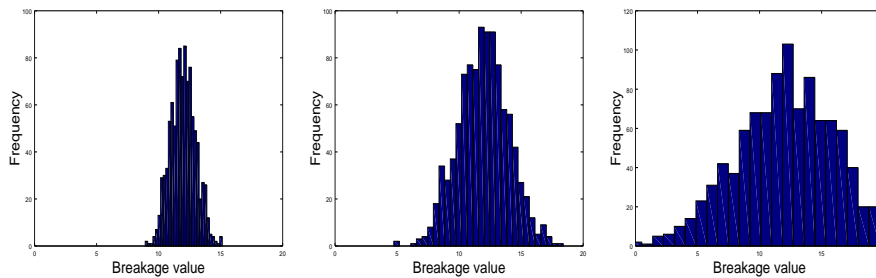


Figure 5: Randomly generated normal distributions of spring breakage tensions for $\sigma = 1, 2, 4$. Left to right - decreasing brittleness. $N = 1000$ springs/bonds.

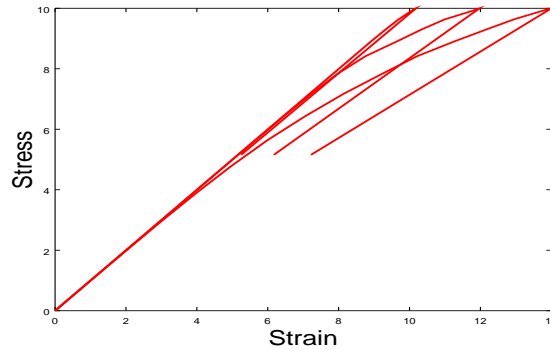


Figure 6: Stress-strain curves from the randomly simulated distributions in Figure 5. Less brittle implies wider curve. The results agree well with Class II materials, but Class I ‘plastic’ behaviour isn’t observed.

behaviour. Further consideration of this approach may yield curves that follow that situation, but this was not considered at MISG, and is the subject of further work.

The dynamic extension: some thoughts

Simple adjustments to the above model will probably not work because the real situation is dynamic even in the ‘static’ stress test. Thus the stress/strain curves displayed in Figure 1 can only be obtained by using special experimental techniques. As the yield stress is approached ‘internal’ dynamics takes over²; the strain increases dramatically, or frictional forces dissipate the energy. The springs equation is given by

$$n_0 m \frac{d^2 u}{dt^2} + \nu \frac{dx}{dt} + nkx = \mathcal{T}^{ext}(t),$$

Before the yield condition is reached the spring term balances external forcing but after yield conditions are reached the external force term becomes irrelevant and the frictional term takes over for Class I materials, and the momentum term takes over for Class II materials. Eventually a balance between applied force and ‘elastic stress’ is reached but with a loss in energy in the Class I case, and with an unrecoverable displacement in both cases. Note that again springs break leaving the remainder to take over, but all the n_0 springs carry momentum.

5 A Continuum State Change Model

The above model is limited in application and therefore we considered another approach based on state change and brittleness ideas. The situation envisaged is as shown in Figure 7. Suppose the end of a semi-infinite rock face at $x = 0$ is struck

²The extending cracks release elastic energy that causes further fracturing

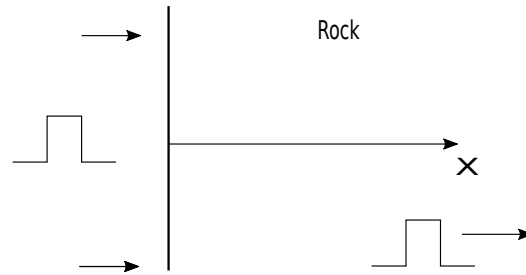


Figure 7: A continuum model of fragmentation. A stress pulse is applied at $x = 0$ to the region $x > 0$. If the pulse strength exceeds the yield stress Y then the material will immediately fail, but otherwise the pulse will propagate into the material.

impulsively. If stress levels generated are less than fracture levels T_{crit} (equivalently Y) then a longitudinal pressure pulse travels away from the face at speed $\sqrt{E_0/\rho}$, and assuming there is no energy dissipation the displacement profile will propagate unchanged.

If, however, stress levels exceed T_{crit} then the rock will partially crush/crack, a situation depicted in Figure 8. Note that in this case the transmitted stress wave is reduced in amplitude due to rock crushing. Under extreme conditions no wave will propagate away from the crushed zone.

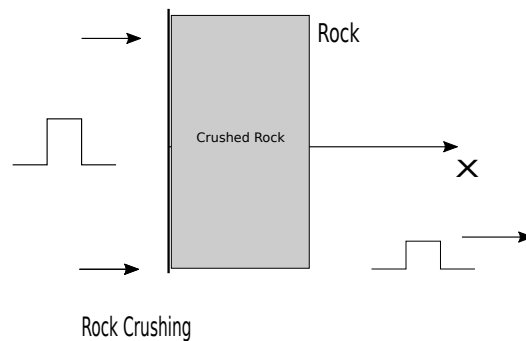


Figure 8: Rock is cracked/crushed by the applied impulse and a weakened pulse continues into the material.

5.1 Equations

If a stress pulse is applied at $x = 0$ then this will result in a propagating pulse into the region $x > 0$ provided the stress at $x = 0$ does not exceed Y . Stress levels greater than Y are not possible because of material failure. With this in mind it is

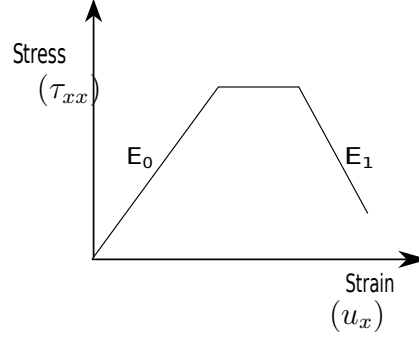


Figure 9: The stress/strain model for the cracking material. In the ductile rock Class I case the effective Young's modulus $E_1 < 0$ beyond the maximum stress point whereas in the brittle rock case Class II case $E_1 > 0$

best to prescribe the displacement at $x = 0$. Cauchy's first law of motion gives

$$\tau_{xx,x} = \rho u_{tt},$$

where $u(x, t)$ is the particle displacement and τ_{xx} is the horizontal stress.

Assuming the impulsive force is uniform and is normal to the face, longitudinal stress waves will be generated and the relevant stress-strain relationship is

$$\tau_{xx} = E^* u_x, \text{ with}$$

$$E^* = \begin{cases} E_1 & \text{for } \tau_{xx} < Y \text{ and } u_x < u_x^1 \\ 0 & \text{for } \tau_{xx} = Y \text{ and } u_x^1 < u_x < u_x^2 \\ E_2 & \text{for } \tau_{xx} < Y \text{ and } u_x > u_x^2 \end{cases}, \quad (10)$$

where we have modelled the stress-strain curve as in Figure 9, and u_x^1 and u_x^2 are strain levels associated with the yield stress $\tau_{xx} = Y$, with $u_x^1 < u_x^2$. Note that E_2 will be either less than zero (the Class II brittle rock case) or greater than zero in the Class I ductile rock case. Now eliminating stress in favour of strain we obtain the equation

$$E^* u_{xx} = \rho u_{tt} \quad (11)$$

where E^* is given by equation (10) for the undamaged, damaged with constant (yield) stress, and damaged regions, respectively.

5.2 Ductile and brittle rocks

Note that across the yielding front the equation changes from elliptic to hyperbolic type for ductile materials, but not for brittle materials in which case the type remains hyperbolic. Thus in the brittle case the energy decays slowly and waves travel

through the front. For ductile materials the impulse is quickly damped. The extent of damage (cracking) can be assessed using a state change idea. The internal energy of the cracked rock is different to that of intact rock. The primary aim of the analysis is to determine the speed of travel of the front, the extent of wave propagation, and the expected fragment size.

5.3 Front conditions

Assume the front moves with speed V (to be determined). A material particle located at x ahead of the advancing front will see the front approaching at speed $-V$. The compressive stress will build up elastically to the yield stress level Y , then rupture will commence and continue until the particle is transformed into its final cracked state. The transition is assumed to be quantified by the stress/strain curve as depicted in Figure 1 with the stress level changing from Y with associated zero strain to the final values corresponding to C in the figure. During this process there will be a change in the internal energy of the particle (due to the opening up of surfaces), again as depicted in the figure with the change dependent on the stored elastic energy and the external work done. As described earlier brittle rocks use the internally stored elastic energy to rupture the material particle, whereas ductile rocks require additional energy from the blast.

6 Conclusions

This is a very difficult problem because the physics is not well understood and it is not clear what form of output would be most useful. What is certainly not required is a complex computational model, even if correct; such a model would be useless in the field requiring too much data input for practical use. The ideal outcome would be a better Kuz-Ram type formula for determining fragment size.

Using scaling ideas we have obtained a formula that is likely to be an improvement on the standard Kuz-Ram model. Certainly the formula is dimensionally consistent, contains essential parameters and it should be equally applicable to small scale laboratory conditions and large scale conditions in quarries and mines. However, there are other parameters that might be chosen, so further substantiation and comparison with data will be required to finalize the appropriate parameters.

A springs model of the fragmentation process has been developed which is encouraging but requires further development to deal with Class II rocks; suggestions have been made for an appropriate model and analysis is underway.

A model based on state change ideas has been suggested which, at least superficially displays behaviour which is encouraging. In particular the model developed exhibits very different behaviour for Class I and Class II rocks and it may turn out that a single formula for fragment size is inadequate. However, with further consideration the ideas considered at the MISG show some promise for finding a

more reliable estimate of fragment size and distribution and developing a better understanding of the processes involved.

References

- [1] Cunningham, C. V. B. (2005). The Kun-Ram fragmentation model-20 years on. Brighton Conference Proceedings 2005, Editors R. Holmberg et al.
- [2] Kulatilake, P. H. S. W., Hudaverdi, T. and Wu, Q. (2012). New prediction models for mean particle size in rock blast fragmentation. *Geotech Geol. Eng.* **30**, 665-684.
- [3] Broberg, K. B. (1999). *Cracks and Fracture*. San Diego Academic Press.
- [4] Zhang, Q. B. and Zhao, J. (2014). Quasi-static and dynamic fracture behaviour of rock materials: phenomena and mechanisms. *Int J. Fract.* **189**, 1-32.
- [5] Li, HB, Lok, TS, Zhou, J. (2005). Dynamic characteristics of granite subjected to intermediate loading rate. *Rock Mech. Rock Eng.* **38**(1), 21-39.
- [6] Tarasov, B. G. and Randolph, M. F. (2011). Superbrittleness of rocks and earthquake activity. *Int. J. Rock Mech. Min. Sci.* **48**, 888-898.
- [7] Tarasov, B. G. and Potvin, Y. (2013). Universal criteria for rock brittleness estimation after triaxial compression. *Int. J. Rock Mech. Min. Sci.* **59**, 57-69.

Appendix A: Dimensional Analysis

The main theorem in dimensional analysis is the Buckingham Pi theorem. An elementary statement of the theorem is as follows.

Consider a physical equation containing n physical quantities (variables and parameters) which depend on k independent dimensions and that $n \geq k+1$. Then the equation can be rewritten in terms of $p = n - k$ dimensionless products, $\Pi_1, \Pi_2, \dots, \Pi_p$, constructed from the original n quantities, as

$$F(\Pi_1, \Pi_2, \dots, \Pi_p) = 0, \quad (\text{A.1})$$

where F is an arbitrary function.

We use dimensional analysis to derive expressions for the mean size x_m .

Consider first the four physical quantities x_m , Y , $\beta\mathcal{E}$ and c_p . The dimensions of these quantities are

$$[x_m] = L, \quad [Y] = \frac{M}{LT^2}, \quad [\beta\mathcal{E}] = \beta \frac{M}{LT^3}, \quad [c_p] = \frac{L}{T}. \quad (\text{A.2})$$

There are therefore three independent dimensions, M , L and T . Thus $n = 4$, $k = 3$ and $p = n - k = 1$. One dimensionless product can therefore be constructed. All dimensionless products are of the form

$$\Pi = x_m^a Y^b (\beta\mathcal{E})^c c_p^d. \quad (\text{A.3})$$

For the product Π to be dimensionless it must satisfy

$$\left[x_m^a Y^b (\beta\mathcal{E})^c c_p^d \right] = M^0 L^0 T^0, \quad (\text{A.4})$$

that is

$$[x_m]^a [Y]^b [\beta\mathcal{E}]^c [c_p]^d = M^0 L^0 T^0, \quad (\text{A.5})$$

which is satisfied provided

$$L^a \left(\frac{M}{LT^2} \right)^b \left(\beta \frac{M}{LT^3} \right)^c \left(\frac{L}{T} \right)^d = M^0 L^0 T^0. \quad (\text{A.6})$$

Equating the exponents of M , L and T gives

$$M : \quad b + c = 0, \quad (\text{A.7})$$

$$L : \quad a - b - c + d = 0, \quad (\text{A.8})$$

$$T : \quad -2b - 3c - d = 0, \quad (\text{A.9})$$

which consists of three equations for the four unknowns a , b , c and d . We solve for b , c and d in terms of a because an expression for x_m is required:

$$b = -a, \quad c = a, \quad d = -a. \quad (\text{A.10})$$

The solution (A.10) can be written in the form of column matrices as

$$\begin{bmatrix} a \\ b \\ c \\ d \end{bmatrix} = a \begin{bmatrix} 1 \\ -1 \\ 1 \\ -1 \end{bmatrix}. \quad (\text{A.11})$$

The right hand side of (A.11) forms a basis for the column matrix on the left hand side. The basis consists of only one column matrix and therefore there is only one dimensionless product, consistent with the Buckingham Pi theorem. Since Π is of the form (A.3) it follows from (A.11) that

$$\Pi_1 = x_m^1 Y^{-1} (\beta\mathcal{E})^1 c_p^{-1} = \frac{x_m \beta\mathcal{E}}{Y c_p}. \quad (\text{A.12})$$

By the Buckingham Pi theorem the original physical equation can therefore be rewritten as

$$F\left(\frac{x_m \beta \mathcal{E}}{Y c_p}\right) = 0, \quad (\text{A.13})$$

where F is an arbitrary function. Since equation (A.13) is satisfied for all values of Π_1 it follows that Π_1 must be a constant. Hence

$$x_m = A \frac{Y c_p}{\beta \mathcal{E}}, \quad (\text{A.14})$$

where A is a constant. In the derivation of (A.14) in Section 3 the form of x_m as a product of powers of Y , $\beta \mathcal{E}$ and c_p was assumed. We see that the form (A.14) follows from the Buckingham Pi theorem. In general, when $n = k + 1$, any one of the n quantities can be expressed as a product of the other $n - 1$ quantities raised to appropriate powers to give the correct dimension. The expression (A.14) does not contain an arbitrary function.

Consider next the five physical quantities, x_m , Y , $\beta \mathcal{E}$, ρ and c_p where the density ρ replaces c_p as one of the four physical quantities thought to be primary. Then $n = 5$ and since

$$[\rho] = \frac{M}{L^3} \quad (\text{A.15})$$

there are still three independent dimensions and $k = 3$. Thus $p = n - k = 2$ and two dimensionless products can be constructed. All dimensionless products are of the form

$$\Pi = x_m^a Y^b (\beta \mathcal{E})^c \rho^d c_p^e. \quad (\text{A.16})$$

For the product Π to be dimensionless it is necessary that

$$[x_m]^a [Y]^b [\beta \mathcal{E}]^c [\rho]^d (c_p)^e = M^0 L^0 T^0. \quad (\text{A.17})$$

and therefore that

$$L^a \left(\frac{M}{LT^2}\right)^b \left(\beta \frac{M}{LT^3}\right)^c \left(\frac{M}{L^3}\right)^d \left(\frac{L}{T}\right)^e = M^0 L^0 T^0. \quad (\text{A.18})$$

By equating the exponents of M , L and T in (A.18) we obtain

$$M : \quad b + c + d = 0, \quad (\text{A.19})$$

$$L : \quad a - b - c - 3d + e = 0, \quad (\text{A.20})$$

$$T : \quad -2b - 3c - e = 0, \quad (\text{A.21})$$

which consists of three equations for five unknowns. We solve for b , c and d in terms of a and e :

$$b = -\frac{3}{2} a - \frac{1}{2} e, \quad c = a, \quad d = \frac{1}{2} a + \frac{1}{2} e. \quad (\text{A.22})$$

Expressed in matrix form the solution (A.22) is

$$\begin{bmatrix} a \\ b \\ c \\ d \\ e \end{bmatrix} = a \begin{bmatrix} 3 \\ -\frac{3}{2} \\ 1 \\ \frac{1}{2} \\ 0 \end{bmatrix} + e \begin{bmatrix} 0 \\ \frac{1}{2} \\ 0 \\ \frac{1}{2} \\ 1 \end{bmatrix}. \quad (\text{A.23})$$

The right hand side of (A.23) forms a basis of two independent column matrices for the column matrix on the left hand side. There are therefore two dimensionless products, consistent with the Buckingham Pi theorem. Since the dimensionless products are of the form (A.16) it follows from (A.23) that

$$\Pi_1 = \frac{x_m \beta \mathcal{E} \rho^{1/2}}{Y^{3/2}}, \quad \Pi_2 = \frac{c_p \rho^{1/2}}{Y^{1/2}}. \quad (\text{A.24})$$

By the Buckingham Pi theorem the original physical equation can be written as

$$F(\Pi_1, \Pi_2) = 0, \quad (\text{A.25})$$

or equivalently as

$$\Pi_1 = f(\Pi_2), \quad (\text{A.26})$$

where f is an arbitrary function. Hence

$$x_m = \frac{Y^{3/2}}{\beta \mathcal{E} \rho^{1/2}} f\left(\frac{c_p \rho^{1/2}}{Y^{1/2}}\right). \quad (\text{A.27})$$

When there are only the four physical quantities, x_m , Y , $\beta \mathcal{E}$ and ρ , there is only one dimensional product and (A.27) becomes

$$x_m = A \frac{Y^{3/2}}{(\beta \mathcal{E}) \rho^{1/2}}, \quad (\text{A.28})$$

where A is a constant.

Finally, consider the seven quantities

$$x_m, \quad Y, \quad \beta \mathcal{E}, \quad c_p, \quad \Delta t, \quad B, \quad J,$$

where Δt is the time delay between charge ignition, B is the spacing between charges and J is the rock joint spacing. The quantities Δt , B and c_p are regarded as independent although a delay time of $\Delta t = B/c_p$ is sometimes used in practice. Since

$$[\Delta t] = T, \quad [B] = L, \quad [J] = L, \quad (\text{A.29})$$

there is still three independent dimensions. Thus $n = 7$, $k = 3$ and $p = n - k = 4$. Four dimensionless products can be constructed. All dimensionless products are of the form

$$\Pi = x_m^a Y^b (\beta \mathcal{E})^c c_p^d (\Delta t)^e B^f J^g. \quad (\text{A.30})$$

The product Π is dimensionless provided

$$[x_m]^a [Y]^b [\beta \mathcal{E}]^c [c_p]^d [\Delta t]^e [B]^f [J]^g = M^0 L^0 T^0, \quad (\text{A.31})$$

that is provided

$$L^a \left(\frac{M}{LT^2} \right)^b \left(\beta \frac{M}{LT^3} \right)^c \left(\frac{L}{T} \right)^d T^e L^f L^g = M^0 L^0 T^0. \quad (\text{A.32})$$

Equating the exponents of M , L and T gives

$$M: \quad b + c = 0, \quad (\text{A.33})$$

$$L: \quad a - b - c + d + f + g = 0, \quad (\text{A.34})$$

$$T: \quad -2b - 3c - d + e = 0. \quad (\text{A.35})$$

There are three equations for seven unknowns which are solved for b , c and d in terms of a , f , g and e :

$$b = -a - f - g + e, \quad c = a + f + g - e, \quad d = -a - f - g. \quad (\text{A.36})$$

Written in matrix form the solution (A.36) is

$$\begin{bmatrix} a \\ b \\ c \\ d \\ e \\ f \\ g \end{bmatrix} = a \begin{bmatrix} 1 \\ -1 \\ 1 \\ -1 \\ 0 \\ 0 \\ 0 \end{bmatrix} + e \begin{bmatrix} 0 \\ 1 \\ -1 \\ 0 \\ 1 \\ 0 \\ 0 \end{bmatrix} + f \begin{bmatrix} 0 \\ -1 \\ 1 \\ -1 \\ 0 \\ 1 \\ 0 \end{bmatrix} + g \begin{bmatrix} 0 \\ -1 \\ 1 \\ -1 \\ 0 \\ 0 \\ 1 \end{bmatrix}. \quad (\text{A.37})$$

The right hand side of (A.37) forms a basis of four independent column matrices for the column matrix on the left hand side. Hence there are four dimensionless products in agreement with the Buckingham Pi theorem. It follows from (A.30) and (A.37) that the dimensionless products are:

$$\Pi_1 = \frac{x_m \beta \mathcal{E}}{Y c_p}, \quad \Pi_2 = \frac{Y}{\beta \mathcal{E} \Delta t}, \quad \Pi_3 = \frac{\beta \mathcal{E} B}{Y c_p}, \quad \Pi_4 = \frac{\beta \mathcal{E} J}{Y c_p}. \quad (\text{A.38})$$

Instead of the dimensionless products Π_3 and Π_4 we work with the dimensionless products Π_3^* and Π_4^* , the physical significance of which are clearer:

$$\Pi_3^* = \frac{\Pi_3}{\Pi_4} = \frac{B}{J}, \quad \Pi_4^* = \frac{1}{\Pi_2 \Pi_3} = \frac{c_p \Delta t}{B}. \quad (\text{A.39})$$

By the Buckingham Pi theorem the original physical equation can be written as

$$F(\Pi_1, \Pi_2, \Pi_3^*, \Pi_4^*) = 0, \quad (\text{A.40})$$

or equivalently as

$$\Pi_1 = f(\Pi_3^*, \Pi_4^*, \Pi_2), \quad (\text{A.41})$$

where f is an arbitrary function. Hence

$$x_m = \frac{Y c_p}{\beta \mathcal{E}} f\left(\frac{B}{J}, \frac{c_p \Delta t}{B}, \frac{Y}{\beta \mathcal{E} \Delta t}\right). \quad (\text{A.42})$$

If the rock joint spacing, J , is not included as one of the physical quantities then there are three dimensionless products and

$$x_m = \frac{Y c_p}{\beta \mathcal{E}} f\left(\frac{c_p \Delta t}{B}, \frac{Y}{\beta \mathcal{E} \Delta t}\right). \quad (\text{A.43})$$

In both (A.42) and (A.43) we see that the length $c_p \Delta t$, which sometimes is chosen to equal B in practice, occurs naturally in a dimensionless ratio with B .